



Research article

Coalescence judgment criteria for the interaction between two close surface cracks by WES2805 and its safety margin for brittle fracture assessment

Tomoya Kawabata ^{1,*}, Shuji Aihara ¹, and Yukito Hagihara ²

¹ Department of Systems Innovation, The University of Tokyo, Tokyo 113-8656, Japan

² Formerly Sophia University, Japan

* **Correspondence:** Email: kawabata@fract.t.u-tokyo.ac.jp.

Abstract: It is important to consider the interaction between multiple cracks in evaluating the reliability of a structure. In this study, the stress intensity factor (K value) is evaluated using the finite element method for interacting surface cracks. Although there are an infinite number of possible conditions of the locations and sizes of two close cracks, the cracks shall be located parallel to each other and have the same dimensions for simplification in this study. The K values on the crack front are calculated under various aspect ratios and relative locations. When there is a strong interaction ($\Delta K_{\max} \geq 10\%$), fracture analysis is generally performed after the coalescence of the two cracks by the FFS standard. As a result of the investigation of the critical condition of the positional parameters for coalescence, judgement criteria were introduced in WES2805 with some simplification. It was revealed that the coalescence process in WES2805 provides a safety margin.

Keywords: stress intensity factor; finite element method; interaction; aspect ratio; safety margin

1. Introduction

Methods to evaluate the soundness of a structure against inherent defects include the Boiler and Pressure Vessel Code Section XI from ASME (American Society of Mechanical Engineers) [1] and the JSME (Japan Society of Mechanical Engineers) Codes for Nuclear Power Generation Facilities [2]. For the soundness of welded joints, WES2805 (Japanese Welding Engineering Society) [3] and BS7910 (British Standard) [4] are representative codes. These types of codes are

called FFS (Fitness-for-Service) codes and have been established as national standards in many countries [5]. In FFS standards, a normalization process for defects is important because real defects have various and complicated shapes, making it impossible to assess the individual stress intensity factor. Coalescence judgements are also important for multiple defects located in close proximity. In many codes, coalescence judgments are incorporated. In the case that multiple cracks are located in adjacent positions, the probability of fracture or fatigue is likely to increase, and defect size must be estimated to be larger than in the case of a single crack. In each standard, the judgment for interaction is assessed mainly by two steps. One is the judgment of alignment for cracks in different parallel plane to be treated as co-planar cracks. Second is the judgment for coalescence for two co-planar cracks to be regarded as one larger crack. It is interesting that these procedures are varied by countries or technical fields. Although an entirely detailed description is impossible due to limitations of space, here some characteristic points of several standards will be described on the basis of the organization by Hasegawa et al. [6]. For the alignment condition, constant critical distance between parallel planes, 12.5 mm, is adopted in ASME, JSME and HPIS. On the other hand, the critical distance is varied with the size of cracks in BS and WES. For example, two surface cracks which is having semi-circular shape is assumed, critical distance is double of the radius of the size of crack in BS and same size in WES (1997) and one and a half times in WES (2007). Thus there is the case the FFS assessment result will vary substantially by the difference of using standards. Coalescence judgment condition of co-planar cracks is also varied by standards. If semi-elliptical surface cracks are assumed in same plane, the critical proximity distance which is needed to be coalesced is determined by crack representative length in all standards. However, which length is used for the judgment is different from standards. The depth of the crack is used in ASME, JSME and HPIS and length is used in BS and WES. Furthermore, BS has characteristic judgement rule, that is, critical proximity distance is varied by the aspect ratio of the cracks. Revised WES (2007) based on this study also has similar characteristic rule.

In general, the stress intensity factor (K value) is used for the establishment of such judgment conditions. In past investigations, an interaction effect has been reported for through-thickness multiple cracks that are regularly located in plane [7,8,9] and parallel [10,11]. The interaction of surface cracks has also been investigated. In general, the profile of the K value of a surface crack is much changed by its aspect ratio, so the interaction of two close cracks becomes more complicated. Several typical problems have been studied so far, including multiple surface cracks located on one line [12–18] and those that are located in parallel but on different planes [19]. However, a quantitative interaction condition has not yet been developed.

Considering such background, some of the authors investigated the increase of K value in the most important situation for welded joints, that is, two surface cracks locate in close position in order to improve the coalescence judgment criterion of WES [20,21]. By these findings and more discussion, for more simplification of criterion considering wide use and the confirmation of the absence of unsafe case WES was revised in 2007. In this paper, K calculations of various combinations of cracks are re-arranged and new calculations for the discussion of revision of WES2805 are shown. Finally a coalescence criterion was clarified especially for brittle fracture. Furthermore, the appropriateness of the coalescence judgement in new WES2805 (in which the findings of this study were already introduced) is investigated.

2. Method

In order to quantify the amount of interaction of two close cracks, finite element method is used as same as the previous researches. The calculations are conducted using ABAQUS (ver. 6.5.1) [22], which is a general-purpose commercial finite element code. The analysis was conducted under elastic conditions under the normal material constants of the steel at ambient temperature, that is, the Young's modulus, E , is set to be 206 GPa and the Poisson's ratio, ν , is 0.3. Uniform tensile stress, σ_0 is assumed as loading condition and set to be 100 MPa. The stress intensity factor, K value was calculated by conversion from a contour integral around the crack tip, i.e., the J-integral value in three modes (opening, in-plane shear and out-of-plane shear) was first calculated and then converted to the K value by equation (1-1) to (1-3) [23], where the integral path is a sufficiently outer contour for which the contour independence is confirmed and the J integral shows a constant value. To perform a finite element calculation, it is necessary to create a finite element mesh. For the accurate calculation of the K value, it is important to allocate finely divided meshes around the crack tip. Used model and meshes are explained separately in the case of surface cracks and that of through thickness cracks.

$$K_I = \sqrt{\frac{J_I \cdot E}{1 - \nu^2}} \quad (1-1)$$

$$K_{II} = \sqrt{\frac{J_{II} \cdot E}{1 - \nu^2}} \quad (1-2)$$

$$K_{III} = \sqrt{\frac{J_{III} \cdot E}{1 + \nu}} \quad (1-3)$$

2.1. Surface Cracks

Figure 1 shows the crack face plane of a single crack that was handled in this manner. In general, the mesh division of a three-dimensional curved crack tip entails a high degree of difficulty, so there is a greater difficulty in producing a model with multiple cracks located at arbitrary positions in different planes (Figure 2), and when the variable S (the distance between two crack tips) is negative, that is, the overlapping condition, it becomes still more difficult. Therefore, when there are multiple cracks, the unit block (referred to as a part) including a surface crack that was created in accordance with the method proposed by Kamaya et al. [19] was copied to the required position, and then they were non-node-covalently bonded. This time, each node position on the joint surface does not necessarily coincide with that on another part; however, the node set on both joint surfaces continues to exist on a single surface. The deformation of both parts is calculated as each face attempts to not be separated (surface to surface features of ABAQUS). In this manner, complex meshing tasks including a plurality of surface cracks can be replaced by a relatively simple task of creating and joining multiple parts of the unit meshes of a single crack. An example of a mesh that is created in

this manner is shown in Figure 3. Cracks having a complex mesh are very close, without the interaction of two mesh divisions. Ordinary type 8-Node quadratic isoparametric element is used in the analysis.

In the finite element method, it is necessary to create a finite object even for an infinite problem. The reported solutions for high-precision surface cracks assume that each crack is in a semi-infinite plate. Hence, a rectangular solid with dimensions of $2W$, $2B$ and t , as shown in Figure 3, was produced, where W , B , and t are all sufficiently longer than the crack length. According to Kamaya et al. [19], by decreasing each of the three parameters, the crack length to width ratio, c/W , the crack length to the analysis model length ratio c/B and the crack depth to analysis model thickness ratio, a/t , and the calculated K value are asymptotic to the solution of the semi-infinite plate model. It can be concluded that by reducing the values to $c/W = 0.2$, $c/B = 0.1$ and $a/t = 0.08$, the model is approximated to a semi-infinite plate. This time, the planes of each crack is set to be perpendicular to the face of the object and the crack of length $2c$ is equal to 6~12 mm and the crack depth a is 3 mm, whereas the size of the model $2W = t$ is approximately 1000 mm and $2B$ is approximately 2000 mm, so that size parameters are calculated, $c/W = 0.012\sim 0.024$, $c/B = 0.006\sim 0.012$, and $a/t = 0.003$, and it is concluded that the size is sufficient to represent a semi-infinite plate.

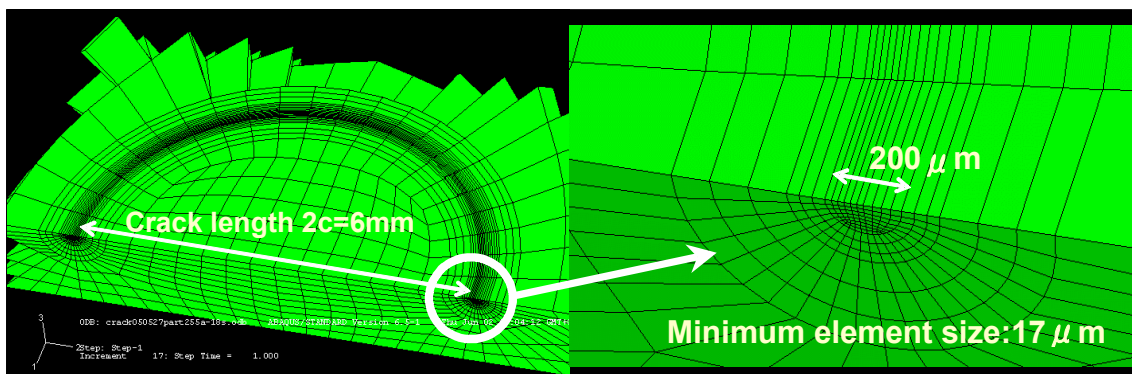


Figure 1. An example of finite element mesh around the crack tip for a semi-elliptical surface crack.

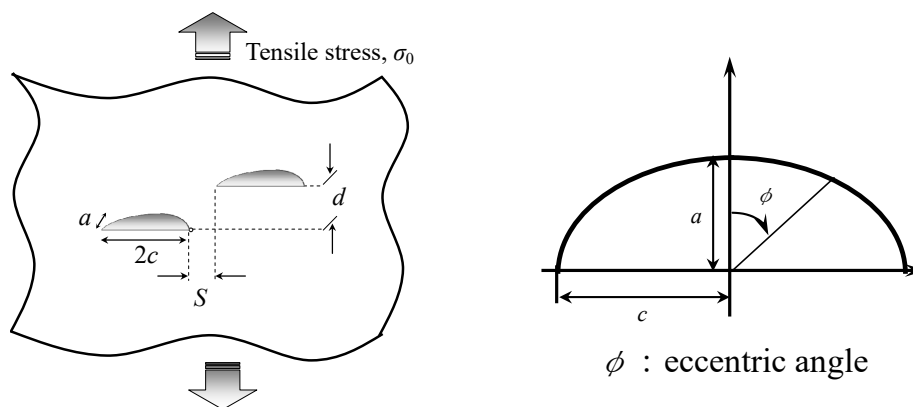


Figure 2. Definition of symbols representing crack location for surface cracks.

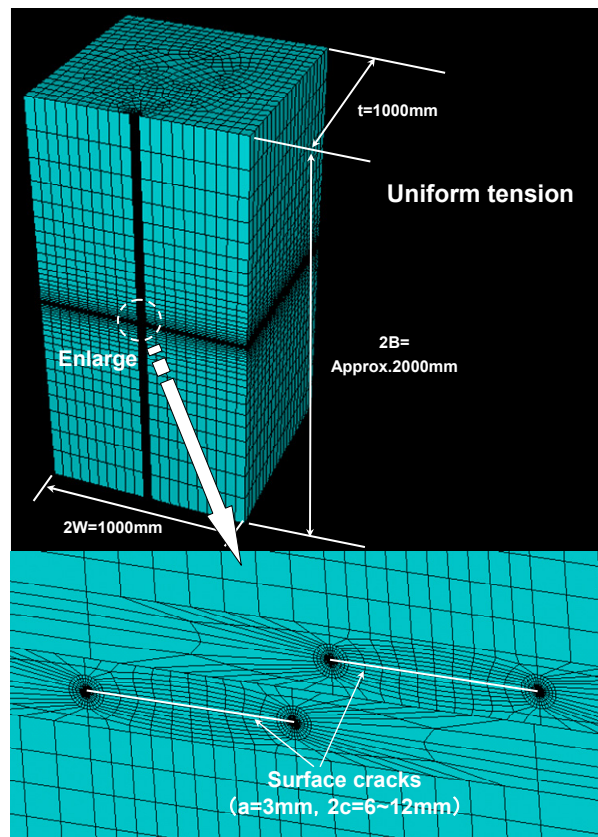


Figure 3. General of whole model for surface cracks.

2.2. Through Thickness Crack

In order to evaluate the extreme high aspect ratio (a/c) condition of the surface cracks, through thickness cracks is modelled in FEM analysis as shown in Figure 4. Two dimensional analyses are conducted by using four nodes-square shape elements accordance with plane strain assumption. Mesh division is easy and unnecessary to use non-node-covalently bonded as surface crack problems. In this study this condition of through thickness cracks is referred as $a/c = \infty$ considering the consistency from the investigation of surface cracks.

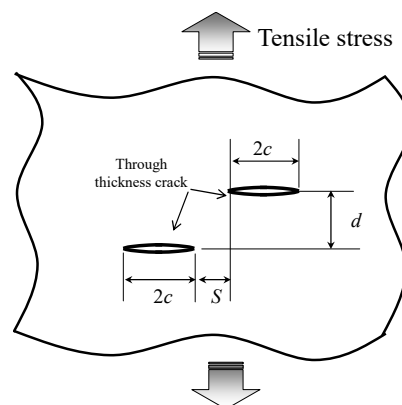


Figure 4. Definition of symbols representing crack location for through thickness cracks.

2.3. Verification of Numerical Analysis

As the analysis of the K values using the finite element method is dependent on the analysis conditions, for example, the element division method, it is essential to verify the analytical accuracy by using an authentic solution result. Here, to validate the analysis accuracy, the K value of a surface crack that exists alone was to be verified by previous literatures in which a high-accuracy solution was reported. The analysis results of the case of a semicircular shape, $a = c = 3$ mm are shown in Figure 4. The K_I value is shown as a dimensionless parameter, the F_I value, by equation (2-1). If only one crack exists under remote uniform stress, both of K_{II} and K_{III} are zero. However, if two cracks are closely located in different planes, K_{II} and K_{III} become to have the positive value. In this section, in order to investigate fracture modes which are needed to be discussed, non-dimensional stress intensity factor, F_{II} , F_{III} are also introduced as shown in equations (2-2) and (2-3), where σ_0 is the uniform tensile stress. Here, there is a need for caution as F_{II} , F_{III} are different from the commonly used non-dimensional parameter. However, authors think that F_{II} , F_{III} can be used for the comparison of the strength of the each stress intensity factor directly.

$$F_I = \frac{K_I}{\sigma_0 \sqrt{\pi c}} \quad (2-1)$$

$$F_{II} = \frac{K_{II}}{\sigma_0 \sqrt{\pi c}} \quad (2-2)$$

$$F_{III} = \frac{K_{III}}{\sigma_0 \sqrt{\pi c}} \quad (2-3)$$

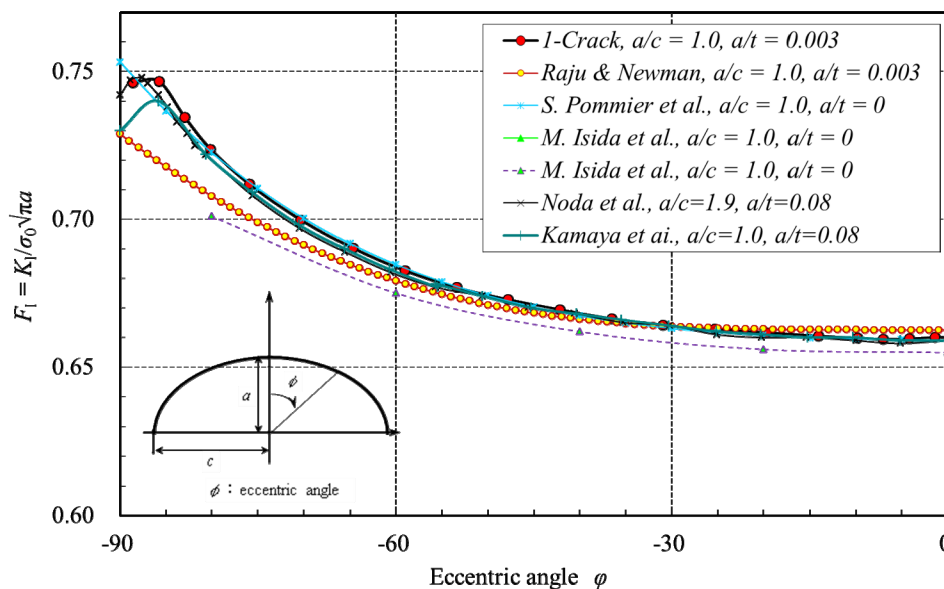


Figure 5. Analytical result of K values of a semi-circular surface crack compared with past studies.

In Figure 5, the results of previous analyses by Newman et al. [24], Noda et al. [25], Kamaya et al. [19], Pommier et al. [26] and Ishida et al. [27] are also shown. The analytical result of this study shows good agreement with that of Noda et al. [25], who analyzed in specific detail the surface portion by the body force method. The analytical results of Noda et al. [25] have a superior feature in that 3 or more digits of precision have been appended.

A similar verification was necessary for a through thickness crack. It is clearly shown in previous paper by authors [20] that the analytical result by the finite element method shows quite good agreement with the theoretical value.

2.4. Importance of Aspect Ratio of a Surface Crack

For the calculation of the K value of a semi-elliptical surface crack, it is important to assess the aspect ratio of the crack. Figure 6 shows the relationship between the aspect ratio and the K value distribution of a single crack by Pommier et al. [26]. In the case where the aspect ratio a/c of the crack is large (deep in the thickness direction), the K value at the end of the surface crack is increased. If it is small (shallow in the thickness direction), the deepest point shows the maximum K value. In discussing an increase in the K value in the case where two surface cracks approach, it is not sufficient to evaluate only the rise in the K value at the closest point, but the maximum K values in the case of a single crack and multiple cracks should also be discussed. Therefore, by calculating the K values in all nodes at the crack tip, the increase in the maximum value was assessed. This is because the maximum K point for multiple cracks is not necessarily at the end or the deepest portion. Additionally, for example, if the aspect ratio a/c is small, although the K value at the proximal end certainly increases even if the surface cracks come closer, it can be assumed that the maximum point is still at the deepest part, and the influence of the interaction that should be taken into account is small.

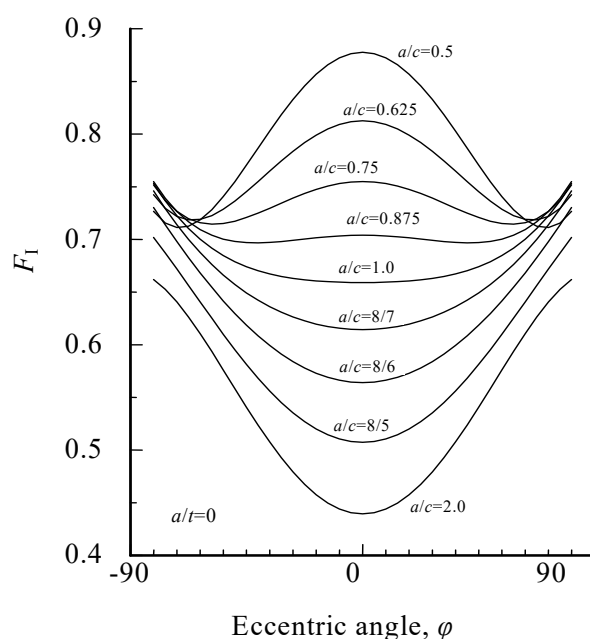


Figure 6. Change of distribution of K values at crack tip of surface cracks with various aspect ratios [26].

In this study, as mentioned previously, the ratio of the maximum K values of a single crack and multiple cracks are discussed by varying the aspect ratio of the crack across 4 levels ($a/c = \infty, 1.0, 0.75, 0.5$), and then the proximity position and the increase in the K value is investigated. The criterion for the interaction was to proceed with the consideration of a K value increase of greater than 10%.

3. Results

3.1. Expression of Proximity Position

In order to discuss the interaction of two close surface cracks having same shape, the positional relationship of two cracks having same shape is expressed based on the coordination of crack tips from the appearance of surface side directly. As shown schematically in Figure 7, one side of crack tips is firstly positioned to the original point. When second crack is considered, the crack tip position which becomes face-to-face is plotted as the expression of the relationship between two surface cracks. In expressing the dimensionless quantities of the proximity distance, S/c and the inter-planar distance d/c were used as the vertical and horizontal axes, respectively. The plot shows the calculation performed at a point in the coordinate system, and the suffix numbers show the index I as the ratio of the maximum value of K_I (Mode I stress intensity factor) in the case of a single crack, $[K_{I,max}]_{single}$ (although there is no maximum or minimum of the concept in the case of through-thickness cracks), to that in the case of multiple cracks, $[K_{I,max}]_{double}$. In sum, I is the percentage increase in the maximum K_I value calculated by equation (3). In this study, the interaction criterion which should be coalesced to one large crack was set to be $I = 10\%$. In this study only mode I is focused. This is because the other stress intensity factor is not considered to be picked up as described in Section 3.2.

$$I = \left(\frac{[K_{I,max}]_{double}}{[K_{I,max}]_{single}} - 1 \right) \times 100 \quad (3)$$

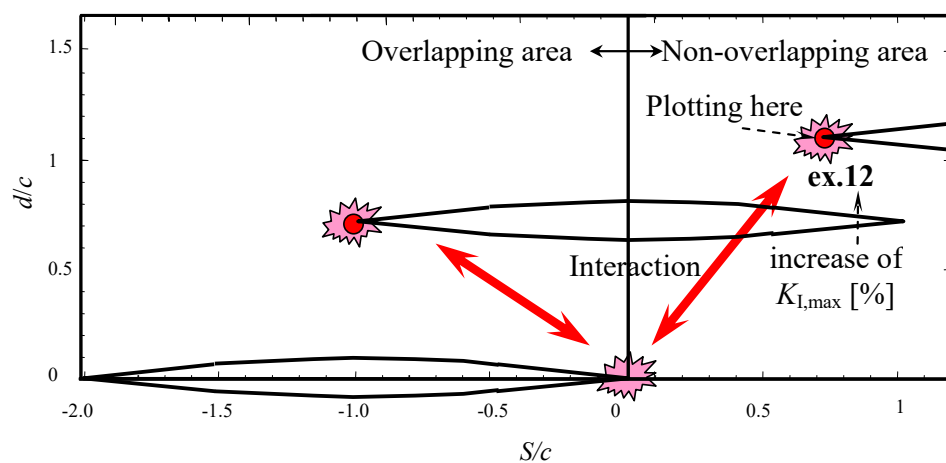


Figure 7. Schematic figure representing the correlation of the coordinates and the actual location of the cracks.

3.2. Fracture Mode for Assessment

To evaluate the interaction in the stress intensity factor when the cracks are present in different planes, as shown in Figures 2 and 3, the stress intensity factor of the shear mode, as well as the opening mode, is clarified. In this study, checking the interaction situation in the three modes for a representative position condition, the mode that has to be investigated is shown. To study the interaction of two identical cracks that are adjacent in the present study, we thought it is beneficial to study a crack shape in which the maximum K_I value is at the end of the crack front, so a semi-elliptical crack with an aspect ratio $a/c = 1.0$ was considered. Considering the case of two cracks with the same dimensions in adjacent positions, their positional relationship is shown in Figure 8. The conditions investigated in this section are the 7 points of A~G in Figure 8. The change in the K value in each mode was expressed by the eccentric angle in Figure 9. It is revealed that Mode I has a significantly greater K value than the others, so the remaining two modes can be ignored.

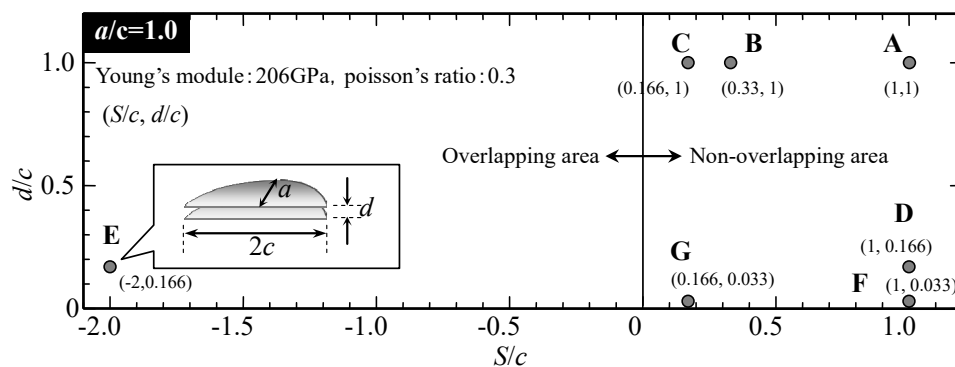


Figure 8. Investigation position for comparison of fracture modes.

3.3. Interaction for Two Close Cracks

Figure 10 shows the calculation results of the case of $a/c = \infty$ as an example. As described in Figure 7, a positive S/c value means that the two cracks do not overlap. When index I is considered in this figure, as the inter-planar distance d/c increases, the interaction amount generally shows a downward trend. However, it is important to note that the maximum interaction point is not necessarily close to the vertical axis, which means that the distance S/c would be equal to zero, but rather the maximum interaction point is moved to a point of distance S/c that becomes larger as the inter-planar distance d/c is increased. This maximum point is considered to correspond to the ridge when drawing stress contours for a single crack (Figure 11). That is, the interaction effect is considered to be maximized when the crack tip of the other surface crack is located at a point corresponding to the ridge of the stress contours. If the interaction is judged as a rectangular solid in the region of $S/c \geq 0$ for this example ($a/c = \infty$), the critical region is $S/c \leq 1.0$ and $d/c \leq 1.5$ by the interpolated calculations. These criteria for through-thickness cracks are wider than those of WES2805-1997 and were adopted in the revision of WES2805 in 2007 and 2011.

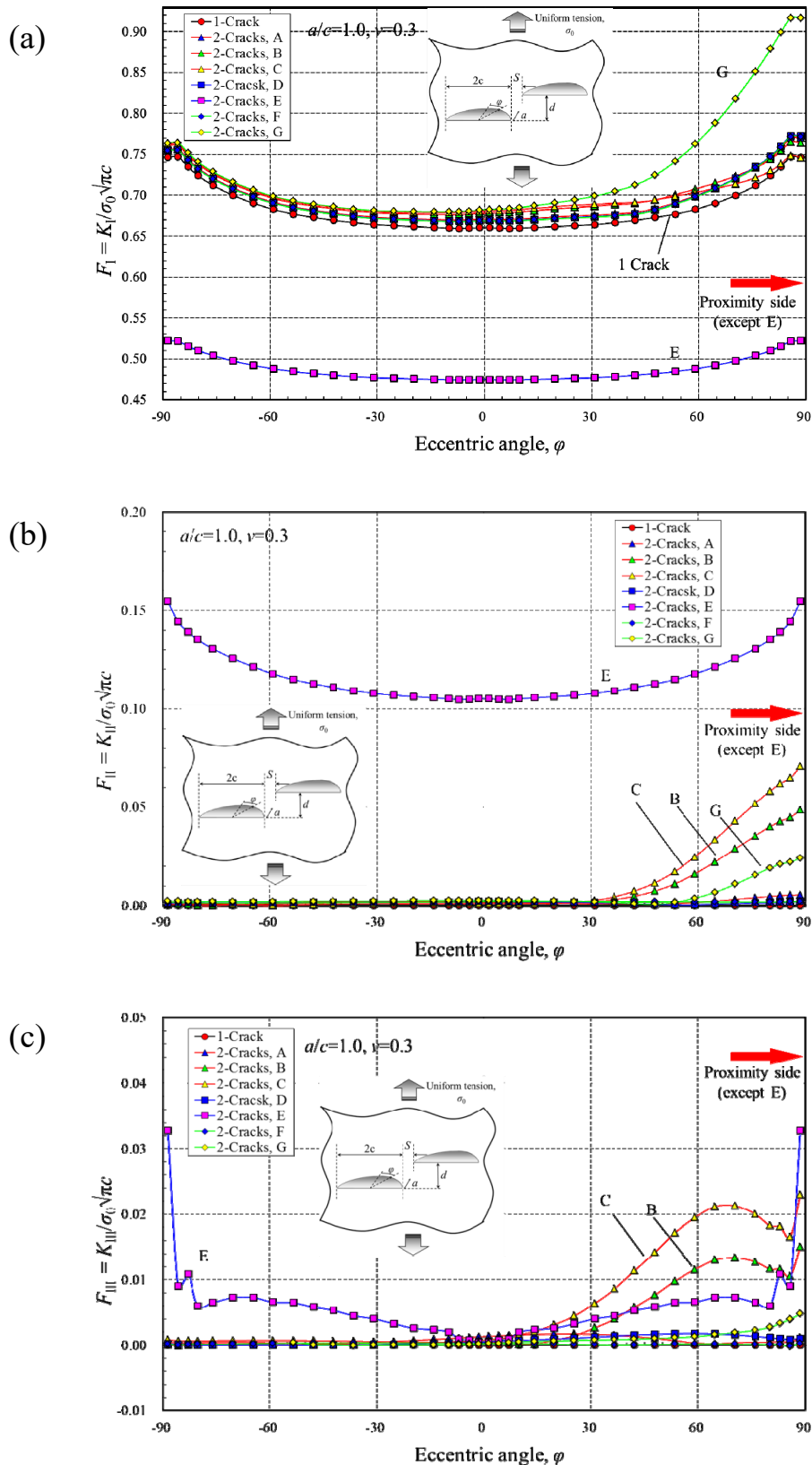


Figure 9. Distribution of non-dimensional stress intensity factors in three modes for two close cracks with low aspect ratio. (a) Mode I Opening, (b) Mode II In-plane shear, (c) Mode III Out-of-plane shear.

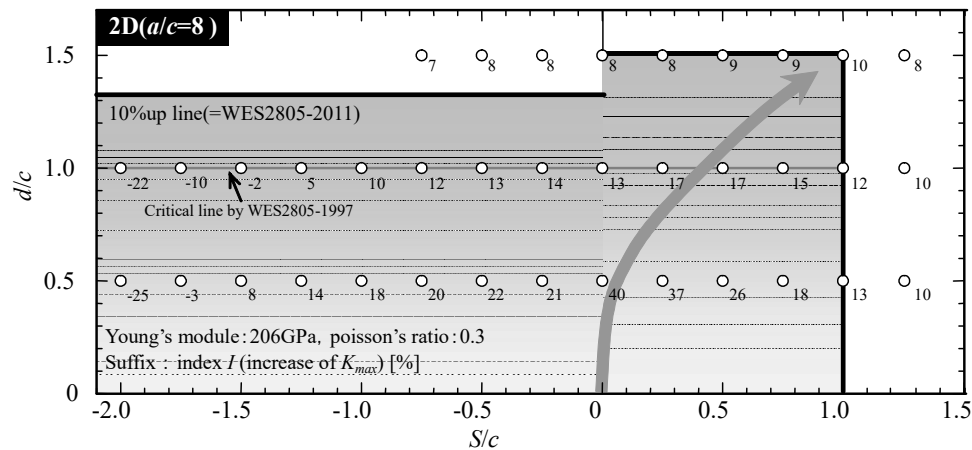


Figure 10. Calculation results of the increase in the maximum K -value of two interacting through thickness cracks ($a/c = \infty$) [20].

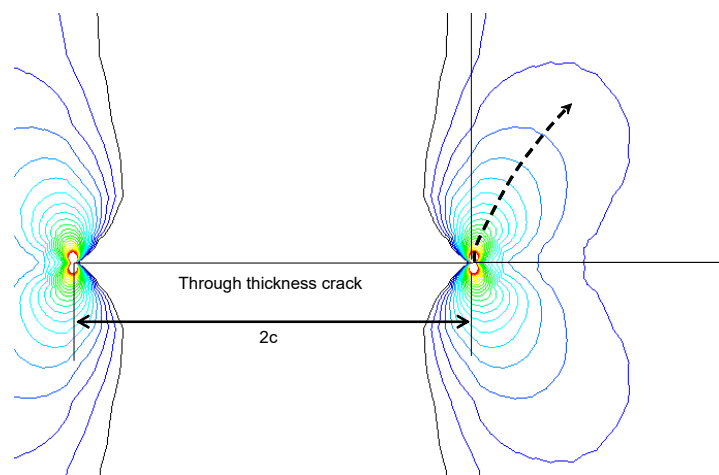


Figure 11. Stress contour line of one through thickness crack under uniform tension.

If S/c is negative, the cracks are located in overlapping positions. Even in this situation, it is clearly shown that the interaction amount becomes smaller at a greater inter-planar distance. The interaction amount decreases to less than zero as the crack approaches the completely overlapping situation, that is, $S/c = -2.0$, and finally at the condition of $S/c = -2.0$ and $d/c = 1.0$, the interaction amount of each crack drops to -22% [20].

In the region of the $S/c < 0$, if the interaction criterion which should be coalesced to one large crack is referred to the inter-planar distance, d/c , $d/c \leq 1.0$ in the case of $a/c = \infty$. Although it is possible to determine the rectangular critical region as being the same as in the condition of $S/c \geq 0$, in this study, only the d/c criterion is adopted, independent of the S/c value. This is because over-conservatism can be avoided when the cracks are located in an overlapping relationship, taking into account that the coalescence procedure adopts an envelope size (Figure 12) for multiple cracks. Finally, the interaction criterion which should be coalesced to one large crack can be expressed as the bold line in Figure 9.

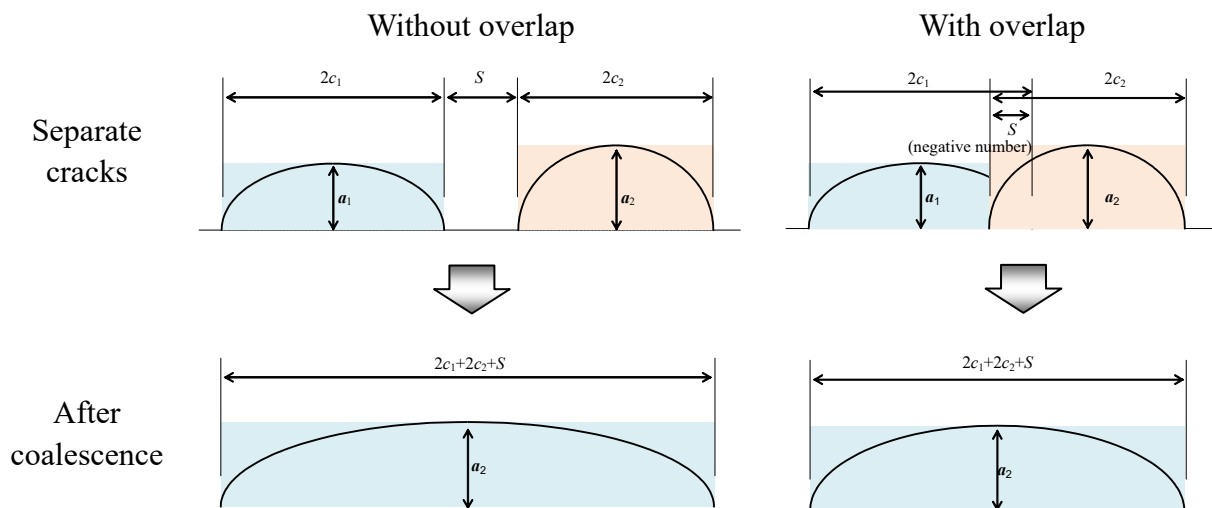


Figure 12. Change of dimensions of interacting cracks by coalescence.

The interaction criterion which should be coalesced to one large crack for the other a/c conditions was also determined by FEM analysis results in a similar way. The result that includes all conditions of a/c is shown in Figure 13. This shows that two cracks with a small a/c condition rarely show interaction. The reason is that the deepest point of the crack with a small a/c condition is the maximum K point, as shown in section 4. Figure 14 shows the interacting situation for very close cracks with $a/c = 0.5$, which indicates that the increase in the K value at the deepest point is not as much as that on the edge. However, the maximum point remains in the deepest point even in this very close case. Even in the case of $a/c = 0.75$, which is almost the same value as between the edge point and the deepest point, the interaction region is so limited in the $S/c \geq 0$ region.

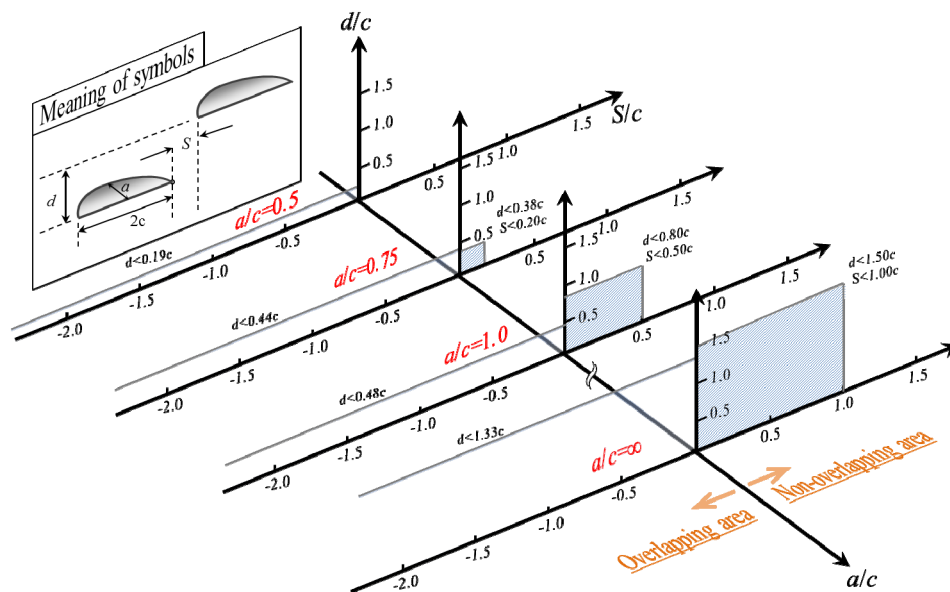


Figure 13. Critical interacting region determined by $I = 10\%$ standard for two semi-circular cracks.

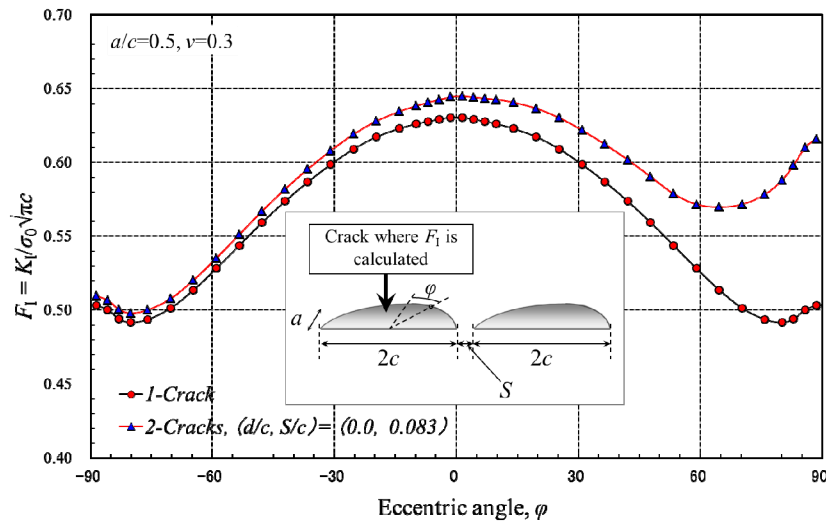


Figure 14. Interaction of very close cracks with $a/c = 0.5$.

4. Discussion

The interaction judgment conditions by the finite element method can be obtained as shown in Figure 13 for each aspect ratio of the crack. In the study of Murakami et al. [13], it was revealed that the K values of a surface crack with a finite a/c value monotonically changes and asymptotically approaches that of the through crack. Hence, a similar tendency is assumed to be maintained for this time interaction conditions, and the results of the surface cracks and through cracks can be thought to have a continuous relationship.

4.1. Non-Overlapping Condition

First, by extracting the critical S/c and d/c value from non-overlapping area in Figure 13, the interaction critical point in the case of $S/c \geq 0$ is plotted as a/c as a vertical axis variable, so the region where coalescence is needed can be recognized in Figure 15. It can be seen from this figure that there is no interaction region in the condition of $a/c < 0.5$. Figure 15 also includes the simplified linear part for such interaction conditions. This relationship can be approximately denoted by equations (4) and (5) for the inter-planar distance d/c and the proximity distance S/c , respectively. If $a/c = \infty$ critical d/c is 1.5 and critical S/c is 1. As explained in previous paragraph, these (Equations (4) and (5) and plots in $a/c = \infty$ condition should be continuously connected so the interaction region becomes representable as a region that is smaller than the dotted line drawn in Figure 15. These critical conditions became reference data for revision activity of WES2805-2011 published by the Japanese Welding Engineering Society. Finally further simplified conditions described as a bold line and arrows in Figure 15 is adopted in the revision. It is clearly shown that the revised WES2805 specification includes much conservatism, especially in the small a/c region. These conservative judgment rules are to avoid complexity and enhance ease-of-use as a fitness for service standard. However, adoption of the judgement that cracks with lower aspect ratio than 0.5 do not need to consider the interaction is quite new and it seems a major advance.

$$d \leq 1.6a - 0.8c \quad (0.5 < a/c \leq 1.5) \quad (4)$$

$$S \leq 1.0a - 0.5c \quad (0.5 < a/c \leq 1.5) \quad (5)$$

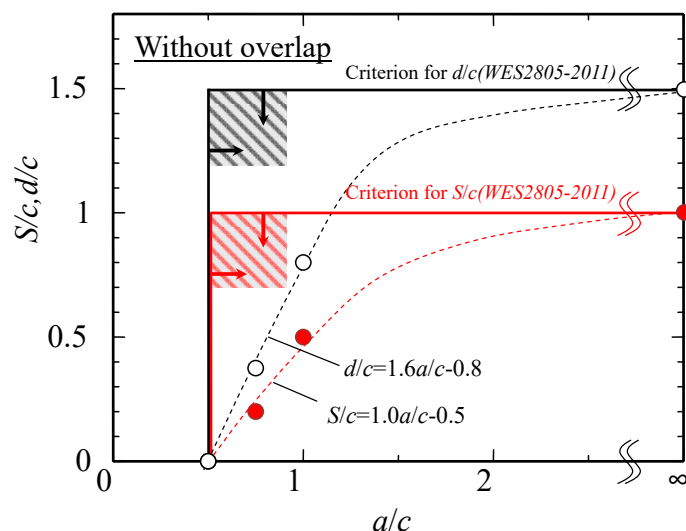


Figure 15. Judgment condition of interaction of two cracks located without overlap.

4.2. Overlapping Condition

In the case of $S/c < 0$, which is the overlapping condition, the critical interacting condition is expressed in a similar way. The approximate critical limit is shown as a dotted line, including the linear part in Figure 16, which is a function of the aspect ratio and independent of S . The linear part can be described as equation (6). In the revised WES2805, the critical condition $d \leq 1.5c$ was adopted as a simplified criterion the same as in the non-overlapping condition. This also includes the conservatism as in the non-overlapping condition. However in overlapping condition, the effect of coalescence treatment is so limited that this conservatism is not thought to come to an issue.

$$d \leq 0.5a \quad (a/c \leq 3.0) \quad (6)$$

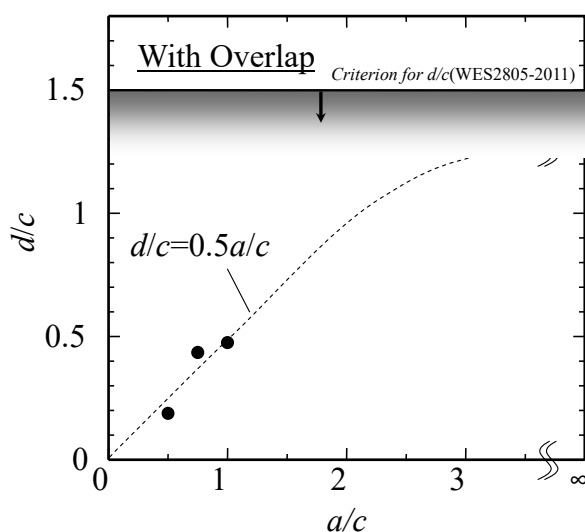


Figure 16. Judgment condition of interaction of two cracks located with overlap.

4.3. Change of K Values by Coalescence Process

Two cracks that satisfy the critical conditions for the interaction are advance through the coalescence process, as shown in Figure 12, which includes some safety margin, as described in the previous section. In this section, it is determined if the increase of $K_{I,max}$ in one coalesced crack compared with one original crack is larger than that of two closely interaction cracks. Figure 17 shows a comparison of the increase of $K_{I,max}$ between one coalesced crack and two cracks in close proximity. Figure 17(a)–(d) correspond to the cases of $a/c = \infty$, 1.0, 0.75 and 0.5, respectively.

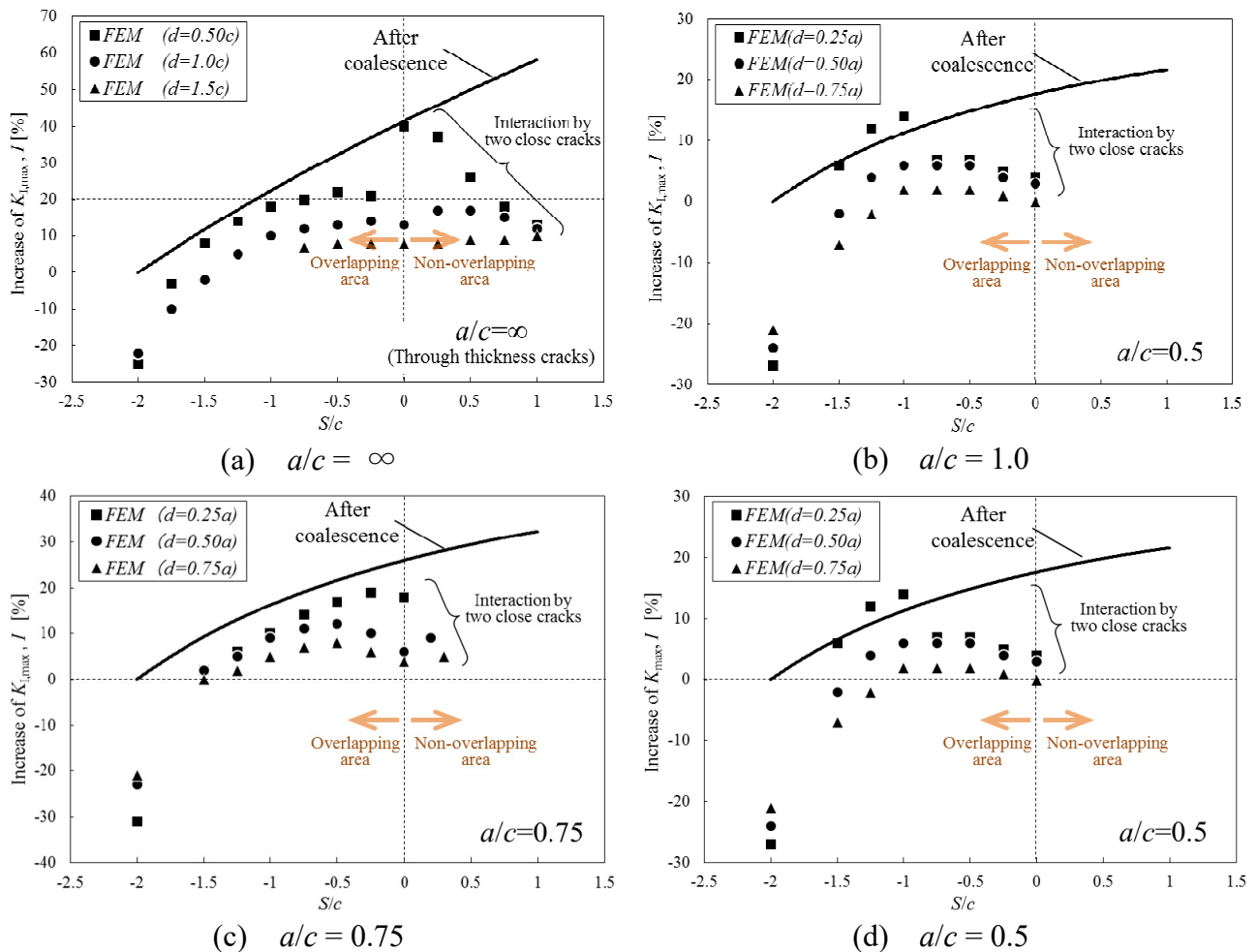


Figure 17. Comparison of $K_{I,max}$ values before coalescence judgement and after.

In this study, in the case of a surface crack, the inter-plane distance is changed to $0.25a$, and in the case of through thickness cracks, the proximity distance between them is changed to $0.50c$. In most cases, the increase of $K_{I,max}$ by the coalescence process exceeds for two interacting cracks. It is intuitive that if the proximity distance is very short, the increase in the $K_{I,max}$ value will rise. Especially in the case of cracks separated by a negligible distance, there may be a large K value at the close side, but brittle fracture generates propagation to combine the two cracks, and then the driving force of the crack is assumed to be able to relax. This means that the increases in the $K_{I,max}$ values at a very close position do not need to be considered. Here, it has been shown that the increase in $K_{I,max}$ in two close cracks almost match with the increase in $K_{I,max}$ by the coalescence process when the

proximity position relationship shows a symbol “■” in Figure 17.

Inter-plane distance of “■”:

- Case(a), through-thickness cracks: $d = 0.5c$;
- Case(b)–(d), surface cracks: $d = 0.25a$.

When the cracks are located in closer proximity than these distances, the coalescence process will result in a prediction that is overly dangerous by WES2805. However, these inter-plane distances are sufficiently short, so the possibility of a brittle crack propagating in a direction different from that of the adjacent crack from the $K_{I,max}$ point is considered to be extremely low. By these considerations, it can be concluded that this envelope process of coalescence provides a prediction that errs on the side of safety.

5. Conclusions

The K value increases due to the interaction of two surface cracks/two through cracks of the same length located in any of the positional relationships were obtained by the finite element method. As a result of a study focusing on the aspect ratio of the crack, the following conclusions were revealed.

- (1) The positional relationship in which the mutual interaction is increased is related to the distribution of the stress contours of the crack tip, not necessarily the point at which the proximity distance is zero.
- (2) In the case of the positional relationship of no overlap ($S/c \geq 0$), the interaction region is greatly affected by the aspect ratio of the cracks. As the shape in the thickness direction becomes deeper, the interaction region increases, and it becomes closer to the interaction conditions of the through-thickness crack. Additionally, in the case of cracks that are shallow in the thickness direction where $a/c \leq 0.5$, the interaction is little seen because the maximum $K_{I,max}$ position is in the deepest part.
- (3) The interaction criterion which should be coalesced to one large crack can be divided into the positional relationship of no overlap ($S/c \geq 0$) and overlap ($S/c < 0$). The region that is judged to be needed to coalesce (a $K_{I,max}$ rise of 10 percent) is approximately notated in Figures 15 and 16.
- (4) These findings were introduced to an FFS standard, WES2805, established by the Japanese Welding Engineering Society (JWES) through some simplification, that is, $d \leq 1.5c$ for overlapping cracks and [$d < 1.5c$ and $S < 1.0c$ and $a/c \geq 0.5$] for non-overlapping cracks. The coalescence procedure adopts the envelope size (Figure 12) of two cracks.
- (5) As a result of the investigation of the safety margin for the coalescence process, it is shown that in the case of close cracks that must be considered to initiate brittle fracture without a short crack to connect two cracks, the increase in $K_{I,max}$ is always higher in one coalesced crack than in two close cracks.

Acknowledgement

The authors wish to acknowledge Iron and Steel Division in Japanese Welding Engineering Society for dedicated discussions of this study.

Conflict of Interest

The authors declare that there is no conflict of interest regarding the publication of this manuscript.

References

1. Boiler & Pressure Vessel Code, Section XI (2015) American Society of Mechanical Engineers.
2. Codes for Nuclear Power Generation Facilities—Rules on Fitness-for-Service for Nuclear Power Plants (2002) The Japan Society of Mechanical Engineers.
3. The Japan Welding Engineering Society (2011) WES2805 (Method of Assessment for Flaws in Fusion Welded Joints with respect to Brittle Fracture and Fatigue Crack Growth).
4. BS7910 Guide to methods for assessing the acceptability of flaws in metallic structures. (2013) British Standards.
5. Hagihara Y (2004) Review of Fitness-For-Service Codes and Standards. *J Jpn Weld Soc* 73: 436–441.
6. Hasegawa K, Miyazaki K (2007) Alignment and Combination Rules on Multiple Flaws in Fitness-for-Service Procedures. *Key Eng Mater* 345–346: 411–416.
7. Ishida M (1969) Stress Intensity Factors in Panels with Cracks in the Same Straight Line. *T Jpn Soc Mech Eng* 35: 1815–1822.
8. Lam KY, Phua SP (1991) Multiple Crack Interaction and Its Effect on Stress Intensity Factor. *Eng Fract Mech* 40: 585–592.
9. Rubinstein AA (1985) Macrocrack Interaction with Semi-infinite Microcrack Array. *Int J Fract* 27: 113–119.
10. Yokobori T (1971) Interaction between Overlapping Parallel Elastic Cracks. *J Jpn Soc Strength Fract Mater* 6: 39–50.
11. Kamaya M (2000) A Crack Growth Evaluation Method Considering Interaction between Multiple Cracks. *T Jpn Soc Mech Eng A* 66: 1491–1497.
12. Murakami Y, Nishitani H (1981) Stress Intensity Factors by interacting of two semi-elliptical surface cracks. *T Jpn Soc Mech Eng* 47: 295–303.
13. Murakami Y, Nemat-Nasser S (1983) Growth and Stability of Interacting Surface Flaws of Arbitrary Shape. *Eng Fract Mech* 17: 193–210.
14. Miyata H, Kusumoto A (1979) Stress Intensity Factors of three dimensional Cracks. *T Jpn Soc Mech Eng A* 45: 252–259.
15. Yoshimura S (1995) New Probabilistic Fracture Mechanics Approach with Neural Network-based Crack Modeling: Its Application to Multiple Cracks Problem. *ASME PVP* 304: 437–442.
16. Noda N (1998) Analysis of Variation of Stress Intensity Factor along Crack Front of Interacting Semi-Elliptical Surface Cracks. *T Jpn Soc Mech Eng A* 64: 879–884.
17. Meessenm O (2000) Applications of Cracked Bricks in Fracture Mechanics : Redustion of ASME Conservatism and Suggestion for ASME Section XI Code Changes. *ASME PVP* 407: 221–228.
18. Miyoshi T (1984) Study on Stress Intensity Factors of Closely Located or Partly Overlapped Twin Surface Cracks. *T Jpn Soc Mech Eng A* 50: 477–482.

19. Kamaya M, Kitamura T (2002) Stress Intensity Factors of Interacting Parallel Surface Cracks. *T Jpn Soc Mech Eng A* 68: 1112–1119.
20. Kawabata T, Konda N, Hagihara Y (2006) Stress Intensity Factors of Two Close Surface Cracks and Their Interaction Criterion. *T Jpn Soc Mech Eng A* 72: 1310–1317.
21. Hagihara Y (2008) Main Points of Revised WES 2805-2007. *J Jpn Weld Soc* 77: 685–688.
22. ABAQUS/Analysis User's Manual Version 6.5 (2000) Hibbitt, Karlsson & Sorensen, Inc.
23. Itoh YZ, Murakami T, Kashiwaya H (1988) Approximate formulae for estimating the j-integral of a circumferentially cracked round bar under tension or torsion. *Eng Fract Mech* 31: 967–975.
24. Newman JC, Raju Jr IS (1981) An Empirical Stress-Intensity Factor Equation for Surface Crack. *Eng Fract Mech* 15: 185–192.
25. Noda NA (2001) Variation of the Stress Intensity Factor along the Crack Front of Interacting Semi-elliptical Surface Cracks. *Arch Appl Mech* 71: 43–52.
26. Pommier S (1999) An Empirical Stress Intensity Factor set of Equations for a Semi-Elliptical Crack in a Semi-Infinite Body Subjected to a Polynomial Stress Distribution. *Int J Fatigue* 21: 243–251.
27. Ishida M (1984) Tension and Bending of Finite Thickness Plates with a Semi-elliptical Surface Crack. *Int J Fract* 26: 157–188.



AIMS Press

© 2016 Tomoya Kawabata, et al., licensee AIMS Press. This is an open access article distributed under the terms of the Creative Commons Attribution License (<http://creativecommons.org/licenses/by/4.0>)